Time-of-flight spectrometer for an ECR ion source

D. R. Whaley and T. P. Goodman

Department of Nuclear Engineering, University of Michigan, Ann Arbor, Michigan 48109

W. D. Getty

Department of Electrical Engineering and Computer Science, University of Michigan, Ann Arbor, Michigan 48109

(Received 12 September 1988; accepted for publication 26 October 1988)

A time-of-flight ion spectrometer using electrostatic grids for ion gating is described. The spectrometer was built to monitor the charge state distribution of endloss ions passing from the midplane region of an ECR-heated, simple magnetic-mirror plasma experiment. Design considerations of the spectrometer are presented as well as the gating pulse circuit and signal amplifier circuit. An example of a time-averaged spectrum is included to illustrate the achievable resolution of the spectrometer. Also a method is described to determine the ion energy distribution of a given charge state in the ion endloss.

INTRODUCTION

Several designs of time-of-flight (TOF) spectrometers have been successfully used to measure ion species present in various plasma devices.[1–3] Recently, interest in the ECR-heated magnetic mirror as a viable source of highly charged ions has developed. Applications for such sources include high-Z ion-beam lithography, cyclotron injection for high-energy physics experiments, and study of multiply charged ion atomic structure.[4] The experiment MIMI[4,5] is an ECR-heated simple mirror device which is being used as a source of multiply charged ions. The ability to measure the charge state distribution of endloss ions is necessary for such an experiment. A time-of-flight spectrometer was chosen for this application over a more complex magnetic spectrometer because of its ability to yield time-resolved spectra in real time and also because of its relative ease of construction and installation, low cost, and light weight. A gridded gating system was chosen because such a system will work properly both in and out of strong axial magnetic fields, unlike the commonly used deflection method[6,7] which can only be used in very low or negligible magnetic fields. Therefore, this spectrometer would be well suited for use in a system in which space limitations require placing the spectrometer close to the region of high magnetic field. (Under these circumstances, ion gyroradius effects must then be taken into account.) The gridded system also allows for measurement of one-dimensional ion endloss energy distributions without the need for additional retarding grids. These distributions are specific to particular charge states. Plasma impurities can be monitored with the spectrometer as well.

I. DESIGN CONSIDERATIONS AND ANALYSIS

A. Spectrometer design

The TOF spectrometer is located in an extension in the north end tank of the Michigan Mirror Machine (MIMI), ~2 m from the plasma on a field line which maps to the magnetic axis at midplane. The plasma is produced by 1 kW of 7.4 GHz ECR microwave power and is limited to a 10-cm diameter and a 50-cm length. Two large end tanks, used for pumping, are located at either end of the 15-cm-diam 150-cm-long tube which contains the plasma. The spectrometer is located in a 10-cm-diam, 1-m extension of the vacuum system in the north end tank.

Schematics of the spectrometer and gating-grid structure are shown in Figs. 1 and 2, respectively. Two 30-cm slots have been machined in the outer grounded tube and 90 1-mm holes have been drilled in the inner high-voltage tube for the purpose of pumping. The holes in the high voltage tube are all located at the front end of the spectrometer since at the front end, the beam of ions is nearest the axis and farthest from any fringing electric fields which may be introduced by the pumping holes. The gating grid of the spectrometer is biased at + 200 V, and the high voltage tube and acceleration grid are biased at − 1250 V. As the plasma impinges on the spectrometer aperture, ions are repelled by the gating grid since they arrive only with energy $E_{\text{ion}} = E_p$

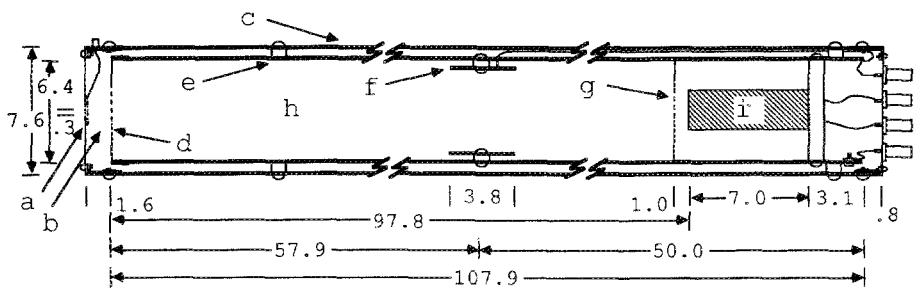

FIG. 1. TOF spectrometer schematic. (a) Gating grid; (b) acceleration region; (c) grounded tube; (d) acceleration grid; (e) high-voltage tube; (f) lens; (g) isolation grid; (h) drift region; (i) ion detector/electron multiplier. Plasma impinges on the entrance aperture from the left. For an expanded view of the entrance aperture/gating grid region, see Fig. 2. All dimensions are in centimeters.

 0034-6748/89/030358-05$01.30

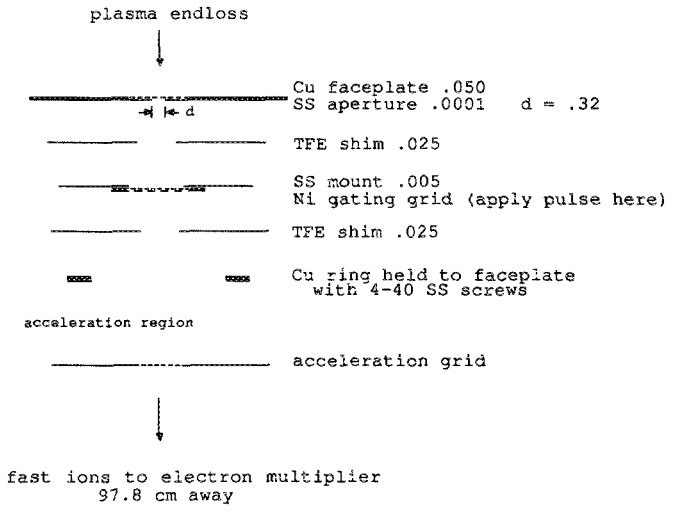

FIG. 2. Entrance aperture/gating grid schematic. All components except the acceleration grid are held tightly together with stainless-steel screws. All dimensions are in centimeters.

$+E_t$, where $E_p = qV_{\text{plasma}}$ and E_t = ion thermal energy. This seldom exceeds 200 q_{ion} eV. The gating grid is composed of Ni mesh that is spot welded to a 5-μm-thick SS mount. The mesh has a 0.25-mm line spacing with 0.035-mm-diam wire. The mesh is located 0.50 mm behind the entrance grid and 10 mm in front of the acceleration grid.

Low-energy electrons are repelled by the acceleration grid, though high-energy electrons with $E_e > 1250$ eV can penetrate into the high-voltage tube. The spectrometer is not magnetically shielded and lies in an axial magnetic field of 45 G at the entrance aperture, which drops to 5 G at the electron multiplier. This magnetic field is used to guide high-energy electrons away from the first dynode of the multiplier. The hot electron population in MIMI has a temperature of 1–3[5] keV. By the time the electrons that leak out of the mirror reach the spectrometer aperture, they have almost purely parallel energy. Therefore, there is a significant population of electrons with energies large enough to penetrate the acceleration (electron repelling) grid. These electrons are still tightly held to the magnetic field lines though the more massive ions are virtually unaffected. The spectrometer is tilted slightly with respect to the magnetic axis so that any field line which passes through the aperture strikes the wall before it reaches the multiplier. This keeps random background noise to a minimum and allows for use of lower acceleration voltages. Secondary electrons due to hot electron bombardment of the high-voltage tube do create some background noise.

A fast, negative pulse typically of 200 V height, 50–400-ns width, with a 20-ns rise time is applied to the gating grid, superimposed on the +200 V bias. The pulse circuit is shown in Fig. 3. This pulse drives the gating-grid voltage to zero and thus provides a brief window in time in which ions can pass through the gating grid unimpeded. This short burst of ions is then accelerated as it passes into the high-voltage tube, and as it drifts the length of the tube the ions separate axially since $v \propto (q/m)^{1/2}$. Ions with the same q/m will arrive at the end of the drift tube at the same time and

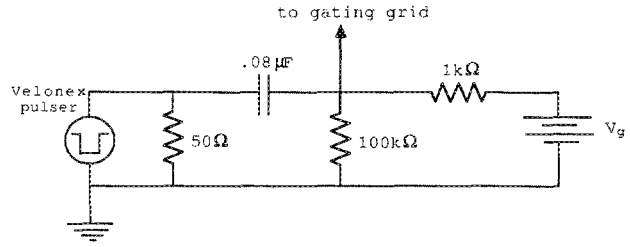

FIG. 3. Gating grid pulse circuit. The pulser is a Velonex model 350-12 fast pulser which has a pulse width of 50–500 ns and rise time of < 20 ns.

can be identified by their time of flight. A lens is located 58 cm down the axis of the spectrometer. It has been shown, both in practice using a segmented collector and in ion trajectory calculations, to be quite effective in focusing the ions onto the electron multiplier at the end of the flight tube. The electron multiplier which amplifies the ion signal is a Vacumetrics AEM-1000 electron multiplier. It is generally operated at 1.5 kV with a resulting gain of $\sim 10^5$. This multiplier was chosen since it uses a dynode material which does not degrade upon exposure to atmosphere. This is important since the spectrometer is frequently removed from the vacuum system. The multiplier is isolated from the drifting region of the high-voltage tube by an isolation grid which has a direct electrical connection to the high-voltage tube. This allows the operator to change the gain of the multiplier without affecting the ion flight times or lens focusing properties.

The signal is then brought out of the vacuum system on TFE insulated RG-196 50-Ω coax cable and terminated in 50 Ω at the input to the signal amplifier. The circuit diagram for the amplifier is shown in Fig. 4. Two amplification stages are necessary to keep the bandwidth of the preamplifier above 7 MHz. This allows a pulse rise time of < 50 ns. (This still, however, limits the response of the electron multiplier which has a rise time of 3 ns.) A line driver is also necessary to enable the amplifier to drive the 50-Ω load at the digitizer used to keep stray capacitance effects to a minimum. The digitizer records the signal from the amplifier and stores it for later processing. The transresistance of the amplifier is 4.7 mV/μA.

B. Gating grid potential calculation

Care must be taken when analyzing the retarding potential of the gating grid. Error will be introduced if the assumption is made that the grid will retard all ions of energy $E_{\text{ion}} < qV_g$, where V_g is the voltage applied to the gating grid. Strong electric fields exist on either side of the grid which have the effect of forcing the potential to droop between grid wires. The magnitude of this droop is a function of the accelerating voltage V_{acc}, the gating-grid voltage V_g, and several characteristic distances as shown in Fig. 5. Constant potentials are assumed on the surface of both the entrance grid and accelerating grid. The potential between wires in the gating-grid plane, as at point X in Fig. 5, is given by[8]

$$V_x \sim \frac{V_g + V_{\text{acc}}/\mu}{1 + (1/\mu)(1 + C_k/C_p)} + \frac{0.105}{n}\left(\left|\frac{V_g}{d_a}\right| + \left|\frac{V_{\text{acc}} - V_g}{d_b}\right|\right), \quad (1)$$

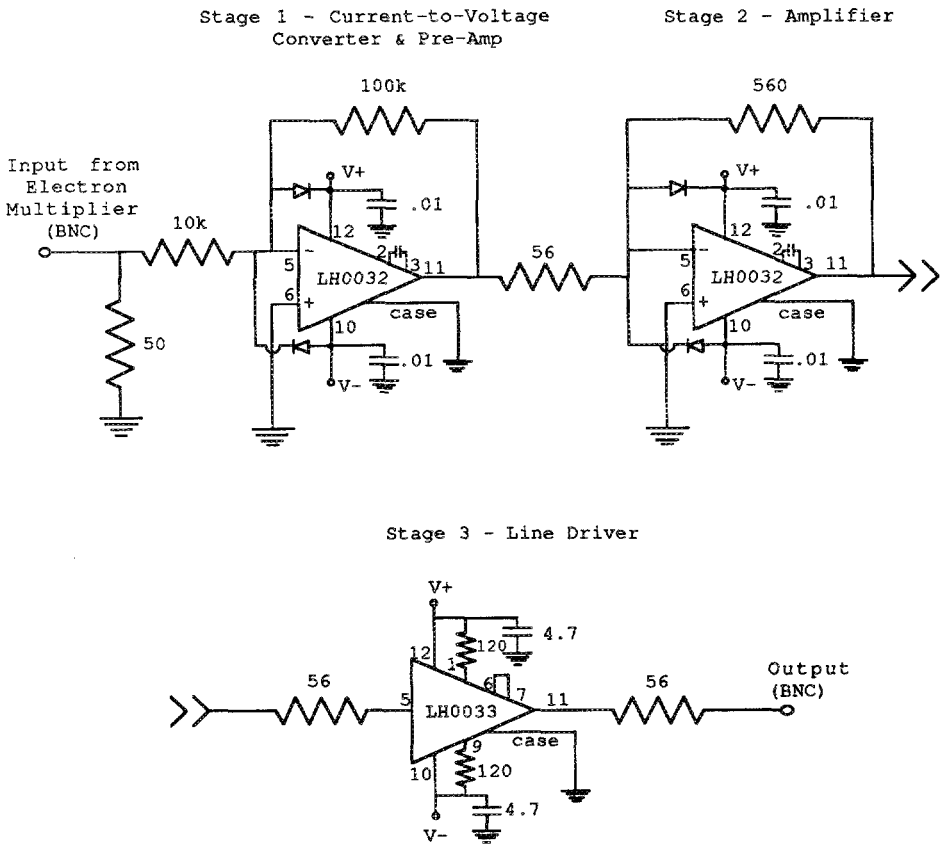

FIG. 4. Amplifier/line driver circuit used to amplify pulses from the electron multiplier of the TOF spectrometer. The output goes directly to a LeCroy model TR8818A transient digitizer. This amplifier has a bandwidth of 7 MHz and a transresistance of 4.7 mV/μA.

where

$$\mu = \frac{2\pi n d_b}{\ln[\coth(2\pi n R)]}$$

$$C_k = \frac{\epsilon_0}{d_a - \dfrac{\ln[\cosh(2\pi n R)]}{2\pi n}}$$

$$C_p = \frac{\epsilon_0}{d_b - \dfrac{\ln[\cosh(2\pi n R)]}{2\pi n}}$$

n = number of lines/m.

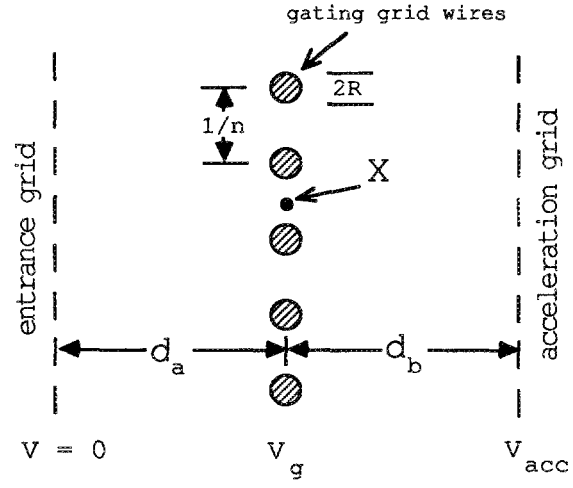

FIG. 5. Expanded view of gating grid region used to calculate voltage droop between gating grid wires.

The dimensions d_a, d_b, and R are defined in Fig. 5. The above expression assumes $V_{\text{aperture}} = 0$, $V_g \geqslant 0$, and $V_{\text{acc}} \leqslant 0$. For the parameters of the MIMI spectrometer and voltages typically used, the voltage droop between the wires of the gating grid is 15%–20% of the gating-grid voltage.

C. Ion energy distribution determination

When the gating grid of the spectrometer is not pulsed but merely holds the repelling dc bias, no ions pass since $E_{\text{ion}} < qV_g$. If the grid is now pulsed to zero, all ions, regardless of energy, may pass through the gating grid into the acceleration region. If, instead, the grid were pulsed to an intermediate voltage V_t, only ions with $E_{\text{ions}} \geqslant qV_t$ could pass. Therefore, a TOF measurement of an ion species using an intermediate gating voltage V_t can be represented as

$$I_{A_i} = \beta \int_{qV_t}^{\infty} F(E_i)\,dE_i\,, \tag{2}$$

where I_{A_i} = collected current of species A of charge state i and β = proportionality constant. It therefore follows that

$$F(qV_t) = F(E_i) \propto -\frac{dI_{A_i}}{dE_i}. \tag{3}$$

Knowing this, the energy distribution of a given charge state can be determined by measuring the current for that charge state as a function of gating-grid voltage during the gating pulse. The energy distribution can then be derived using Eq. (3).

II. DATA PROCESSING AND SAMPLE RESULTS

The output of the amplifier is digitized using a LeCroy TR8818A, 100-MHz transient digitizer. To achieve the desired resolution, a clock speed of at least 50 MHz is required. Since each spectrum requires 20 μs at 20 ns/point, and the digitizer maximum total storage is 128 (1024) points/trace, about 130 spectra can be stored per shot, covering $\sim$2.5 ms of plasma time. A FORTRAN program then averages these spectra to reduce random signal fluctuations due to secondary electron and x-ray bombardment of the multiplier, plasma fluctuations, amplifier noise, etc. This method works quite well and the 100 + spectra that are averaged appear to be a sufficient number to ensure shot-to-shot reproducibility. Also the 2.5 ms that is required to record a set of spectra is a small fraction of the total plasma shot time of 100 ms. The capability then exists to document transients with time constants longer than 2.5 ms. Measurements of this type show typical charge state buildup times of $\sim$10 ms.

A sample spectrum from an argon plasma is shown in Fig. 6. For this spectrum, $V_{HVT} = -1250$ V, $V_{EMT} = -1500$ V, $V_{LENS} = -400$ V, and $V_{plasma} = 100$ V. From this spectrum the resolution of the spectrometer can be estimated to be $(m/q)/\Delta(m/q) \sim 35$. This resolution is sufficient to resolve peaks of charge states of interest for working gases up through krypton, the heaviest gas yet tested. As can be seen, a major contribution to the spectrum comes from impurities—specifically C, O, and H_2O. It is believed that the presence of these impurities in the spectrum is due to plasma bombardment of the vacuum vessel walls during the plasma shot. An RGA spectrum taken before the run confirms background impurities consist primarily of water vapor and rotary pump oil whose major components include H, C, and O.

Figure 7(a) shows data taken from a scan of Ar^{2+} signal amplitude as a function of gating-grid voltage. This applied voltage has been corrected for nonzero line spacing of the gating-grid mesh following the procedure of Sec. I B. The derived energy distribution is shown in Fig. 7(b). The Ar^{2+} ions lie between energies 150 and 270 eV and are evenly distributed in this range.

Ions which produce the spectrometer signal are born in the ionizing region of the plasma, which exists between the hot electron resonance zones near the midplane of the mirror. When a neutral particle is ionized, it has zero energy relative to the potential of the plasma at the location of ionization. When this ion leaves the plasma region, it gains the energy $q_{ion} V_{plasma}$, where V_{plasma} is the plasma potential at its original location of ionization. Since this plasma potential varies over the region of ionization, ions leaving the plasma will have a spread of energies directly resulting from the spread in plasma potential. This spread is evident in Fig. 7(b). The plasma potential range can be deduced from this plot as $70 \text{ V} \leqslant V_{plasma} \leqslant 130 \text{ V}$. An average plasma potential of $\sim$100 V has been confirmed through independent measurement.

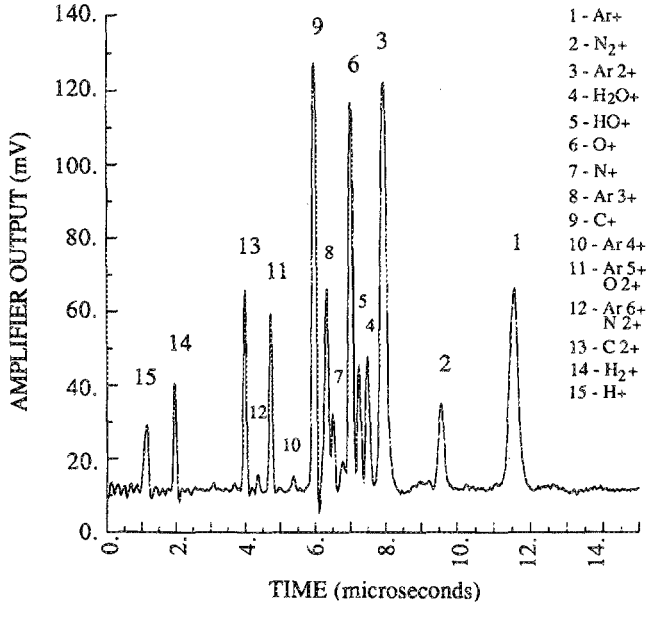

FIG. 6. Average of 130 argon spectra. The impurities are believed to be due to plasma bombardment of vacuum vessel walls contaminated with water vapor and rotary pump oil.

III. DISCUSSION

Design of a gridded time-of-flight ion spectrometer which has yielded good results has been presented. This

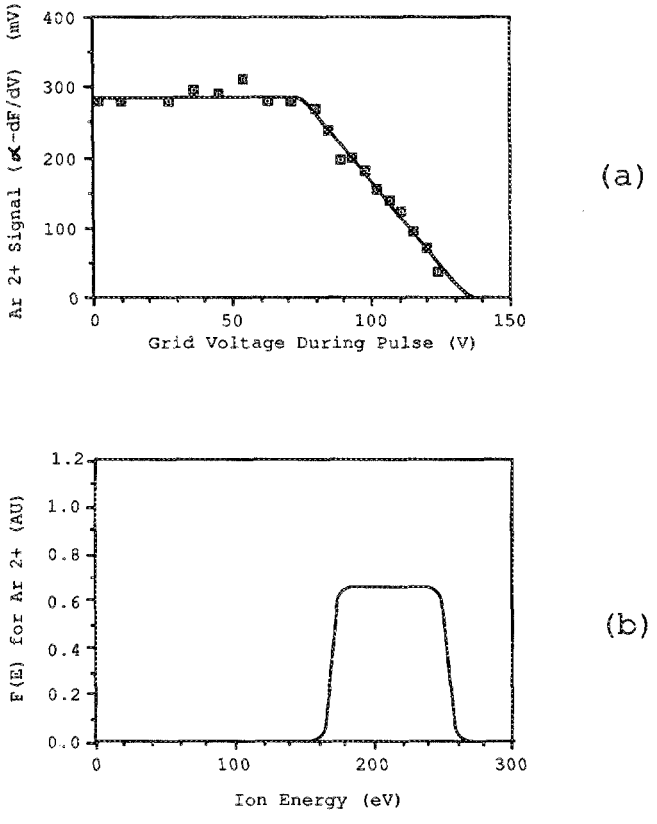

FIG. 7. (a) Ar^{2+} signal vs gating grid voltage at time of pulse. This is a measure of the ion population at or above energy $q(V_g + V_{pulse})$. The gating grid voltage has been corrected for voltage droop due to nonzero line spacing of the gating grid mesh. Note the linear scale on the vertical axis. (b) Derived Ar^{2+} energy distribution. The distribution is primarily determined by the spread in plasma potential in the ionization region of the plasma. Note the change in scale of the horizontal axis from (a) to (b) due to the ion charge.

spectrometer is being used to monitor both impurities and ion charge state distributions of MIMI. The spectrometer employs biased grids to gate and accelerate plasma ions as well as to retard plasma electrons. Also an extra grid is used to isolate the multiplier from the drift region of the spectrometer which allows for independent operation of the multiplier cathode voltage (and therefore multiplier gain) and ion acceleration voltage. A wideband, high transresistance amplifier circuit has been designed and built which satisfies bandwidth, gain, and 50-Ω drive capability requirements. The averaging of many spectra over a small fraction of the plasma pulse is adequate to increase the signal-to-noise ratio to acceptable levels, to reduce random signal fluctuations so that shot-to-shot reproducibility is assured, and to allow for measurement of transients with time constants greater than 2.5 ms. The averaged spectra also show good resolution. A method is presented to determine the energy distribution of a particular ion charge state in the endloss without the need for extra grids or high-voltage power supplies. The distributions are found to be dominated by spread in the plasma potential in the ionizing region of the plasma. Current work is underway to reduce impurity levels in the spectra which can obscure small peaks of highly charged working-gas ions.

ACKNOWLEDGMENTS

The authors would like to thank M. E. Herniter for helpful discussions on programming algorithms and circuit design and also for use of much needed equipment. This work is partially supported by National Science Foundation. D. R. Whaley is supported by the DOE Magnetic Fusion Energy Technology Fellowship program.

[1]M. Krishnan and J. L. Hirshfield, Rev. Sci. Instrum. **51**, 911 (1980).
[2]N. I. Alinovskii, in *Recent Advances in Plasma Diagnostics*, edited by V. T. Tolok (Consultants Bureau, New York, 1971).
[3]J. D. Pinkston, M. Rabb, J. T. Watson, and J. Allison, Rev. Sci. Instrum. **57**, 583 (1986).
[4]J. Booske, F. Aldabe, R. F. Ellis, and W. D. Getty, J. Appl. Phys. **64**, 1055 (1988).
[5]J. H. Booske, W. D. Getty, R. M. Gilgenbach, and R. A. Jong, Phys. Fluids **28**, 3116 (1985).
[6]C. C. Petty, D. K. Smith, and D. L. Smatlak, Rev. Sci. Instrum. **59**, 601 (1988).
[7]I. G. Brown, J. E. Galvin, R. A. MacGill, and R. T. Wright, Rev. Sci. Instrum. **58**, 1589 (1987).
[8]W. G. Dow, *Fundamentals of Engineering Electronics* (Wiley, New York, 1937).